Pressure Fluctuations in the Tip Region of a Blunt-Tipped Airfoil

S. A. McInerny* and W. C. Meecham†
University of California, Los Angeles, California
and
P. T. Soderman‡
NASA Ames Research Center, Moffett Field, California

The characteristics of turbulence generated in the tip region of a blunt-tipped airfoil were studied using surface pressure measurements. Pressure transducers were located at five chordwise positions on the upper tip-edge, the lower tip-edge, and on the flat tip. The model was an NACA 0012, 0.76-m chord, aspect ratio 2.7, semispan wing section. Tests were performed at flow speeds of 75, 55, and 35 m/s and angles of attack of 6, 12, and 16 deg. Reynolds numbers based on the wing chord were 1.9, 3.0, and 4.1×10^6. Pressure fluctuations measured near the primary tip-vortex on the upper, low pressure side of the wing tip were uncorrelated with those on the blunt tip. Fluctuations on the high pressure side of the wing were strongly correlated with those on the flat tip, but 10–20 dB less intense. Spectra measured on the flat tip displayed pronounced peaks at dimensionless frequencies $ft/U_0 = 0.8$ to 1.3. Cross correlations between some of the flat-tip pressures displayed two echolike groupings. A model is proposed that explains these correlations.

Nomenclature

AR = wing aspect ratio (wing span divided by wing chord)
C_L = wing lift coefficient
C_d = wing drag coefficient
D = diameter of the secondary tip-vortex core
$E(f)$ = *pressure power spectral density in* $(N/m^2)^2/Hz$
f = frequency in Hz
f_p = frequency, in Hz, of peak energy in spectrum or correlation
Δf = bandwidth, in Hz, of energy in a cross correlation
q_0 = freestream head $(\rho U_0^2/2)$ in. N/m^2
St = Strouhal number, dimensionless frequency, ft/U_0
t = wing thickness in m
t_d = turbulence convection time
U_m = mean streamwise velocity in secondary tip-vortex
U_0 = freestream velocity in m/s
α = wing angle of attack in rad
τ = correlation delay time

Introduction

THE results reported herein were obtained from an experimental study of side-edge flap noise. Turbulent flow over extended flaps and landing gear has been found to be a major source of airframe noise. On flaps, the blunt side edges appear to be the strongest source region.[1-4] A simple airfoil model was chosen so that the basic turbulence mechanisms might be isolated from those due to airframe components and interaction effects. Isolation of the model "flap" from the upstream wing appears to have increased the complexity of the flow in the region of the blunt tip, allowing the formation of more than one well defined, steady tip-vortex. The surprising qualities of the tip turbulence, as reflected in the spectra and cross-correlations, led to an expanded study of the fluctuation pressure field. The findings of that investigation are detailed in this paper.

Tip vortices affect the aerodynamic performance of wings, as well as influence the unsteady loading of nearby surfaces. In the case of rectangular airfoils, the suction pressure generated by excess axial velocities in the tip vortex core provides a lift increment above that predicted by thin airfoil theory.[5] Over delta wings, the breakdown of leading-edge vortices leads to a rapid drop in wing lift and loss of aerodynamic stability. Flow in a three-dimensional vortex is characterized by a circumferential velocity which increases from zero on the vortex axis to a maximum at the vortex core radius. Axial velocities within a vortex core can be greater or less than the freestream velocity. In the former case, the vortex is referred to as jet type, in the latter, wake type.

The results of the present study support the existence of a turbulent, jet-type, *secondary* tip vortex adjacent to the flat airfoil tip in addition to the primary tip vortex on the upper wing surface. The two steady vortices are termed secondary and primary following established terminology.[5-8] The primary tip vortex on the upper (low pressure) side of the wing and the secondary tip vortex opposite the blunt tip are three-dimensional vortices with the same rotational sense.

Although the existence of a secondary vortex opposite the square tip has been established from flow visualization and hot-wire studies,[5-8] little detailed information has been obtained on its structure. An excess axial velocity in the secondary vortex has been inferred from (mean) suction pressure peaks measured where the axis of the secondary vortex crosses the upper wing surface.[7,8] Turbulence convection velocities in excess of the freestream, measured in this study, provide further supporting evidence of excess axial velocities in the secondary tip vortex.

Fluctuating surface pressures measured in this study also lend support to the view[6] that the primary tip vortex begins formation on the upper wing surface (as opposed to opposite the flat tip near the leading edge with a subsequent cross over to the upper surface[5]). Qualitative sketches of the primary and secondary tip-vortex locations and the cross flow in the tip region are given in Fig. 1. The location of the secondary tip

Received April 13, 1988; revision received April 17, 1989.

*Pacific Telesis Senior Fellow. Currently, Assistant Professor, California State University, Long Beach. Member AIAA.
†Professor, Mechanical, Aerospace and Nuclear Engineering Department. Associate Fellow AIAA.
‡Group Leader, Acoustics. Member AIAA.

vortex in this figure was inferred from the results of this study and is consistent with the findings of previous investigators. The location of the primary tip-vortex axis has an extensive empirical basis.[6,7]

It should be noted that the emphasis of this study was on surface pressure cross correlations and spectral analyses. Calibrated turbulence levels were not acquired.

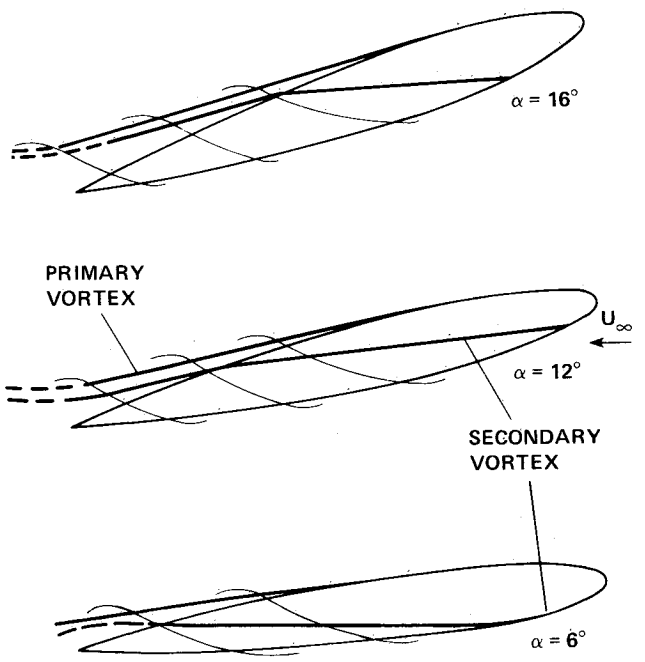

Fig. 1a Qualitative sketch of tip-vortex axis locations, end view.

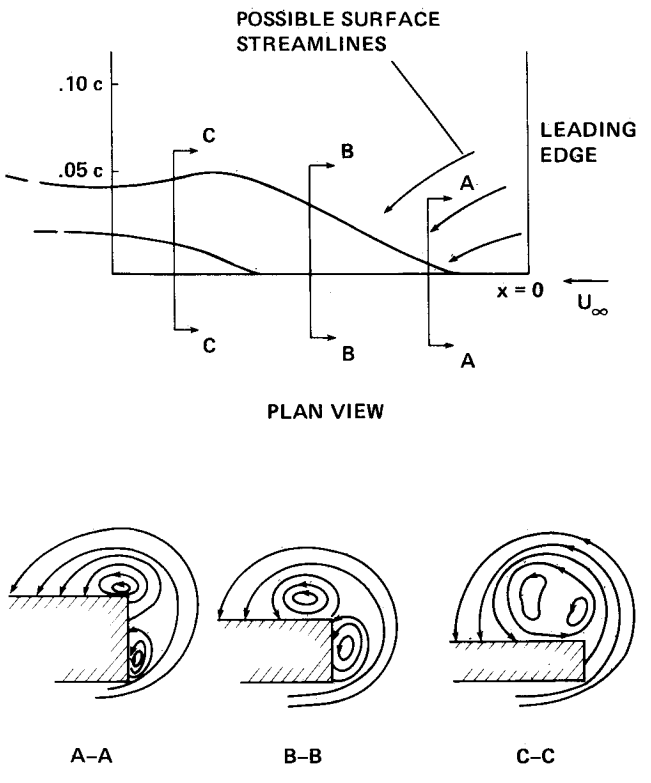

Fig. 1b Qualitative sketch of tip-vortex axis locations, plan view with cross sections (note expanded spanwise scale).

Experiment

Measurements of surface pressure fluctuations were made for wing angles of attack of 6, 12, and 16 deg at flow speeds of 35, 55, and 75 m/s. The Reynolds numbers, based on wing chord, were 1.9×10^6, 3.0×10^6 and 4.1×10^6; the Mach numbers were 0.10, 0.16, and 0.22.

All experiments were performed in a 2.13×3.05 m (7×10 ft) subsonic, wind tunnel at NASA Ames Research Center. The model used was a smooth NACA 0012 wing section with an instrumented tip. The wing chord was 0.76 m, and the floor-to- and the floor-to-tip semispan was 1.01 m (aspect ratio 2.67). The transducer locations and numbering system are shown in Fig. 2. In the cross section of this figure, the design of the transducer mountings and the wiring slot are shown.

Data Acquisition and Reduction

The following is a brief outline of the data acquisition systems used in the experiments. Details can be found in Ref. 9. All fluctuation signals were adjusted to optimal levels and recorded on analog tape for subsequent data processing.

Surface Pressure Transducers

Surface pressure fluctuations were measured with BBN model 377 piezoelectric transducers and recess mounted in slots with sensing ports to the surface. Transducer sensitivities and frequency responses were determined by the NASA Ames Environmental Laboratory. Prior to mounting in the recessed slots, in-line sensitivities were measured with a 124-dB, 250-Hz pistonphone signal. No insitu calibration was devised for the transducers in the mounting slots.

Data Reduction

Surface pressure spectra and cross correlations were calculated on an HP 5420 spectral analyzer. Anti-aliasing filters are an integral part of this analyzer. No additional filtering was required for the determination of power spectral densities (PSD's) and integrated rms pressures. For cross correlations, a Krohn-Hite 3322 filter set was used to high pass the signals and eliminate uncorrelated energy and low-frequency wind-tunnel tones. These wind-tunnel tones presented a problem only in correlations with relatively low-level signals. At a flow speed of 75 m/s, tonal energy centered at frequencies of 330 Hz (corresponding to St 0.4) and 510 Hz (St 0.6) was measured in the spectra of several far-field microphones. The measured PSD levels of these disturbances varied with location in the tunnel but never exceeded a normalized level $[E(f)U_0/q_0^2t]$ of 1.3×10^{-5}. A less prominent tonal disturbance was also noted, centered on 630 Hz (St 0.8), with a peak normalized PSD level of 4.2×10^{-6}.

Cross-correlation analysis was chosen as the primary dual-signal analysis tool. Turbulence convection velocities calculated from cross-spectral phase plots were found to be one-third to one-half those determined from correlation delay times. This discrepancy is attributed to the existence of echo like structures in the correlations. In theory, cross correlations and cross spectra contain the same information. However, accurate phase estimates require either high coherence or a very large number of averages. Echos in a cross correlation can have a disastrous effect on experimental phase information.[10]

Data Presentation

The assumed characteristic variables U_0, t, and $q_0 = (\rho U_0^2/2)$ were used to collapse the spectra for the three flow speeds at each angle of attack. A curve which best fit the dimensionless dependence was then fitted to each set of (three) plots. With few exceptions, the individual curves deviated from this mean by less than 1.0 dB. Where transducer mounting port resonance effects (see Ref. 9) were apparent, the curve was fitted to an individual dimensionless plot (75, 55, or 35 m/s) considered to be resonance free. Such regions of the

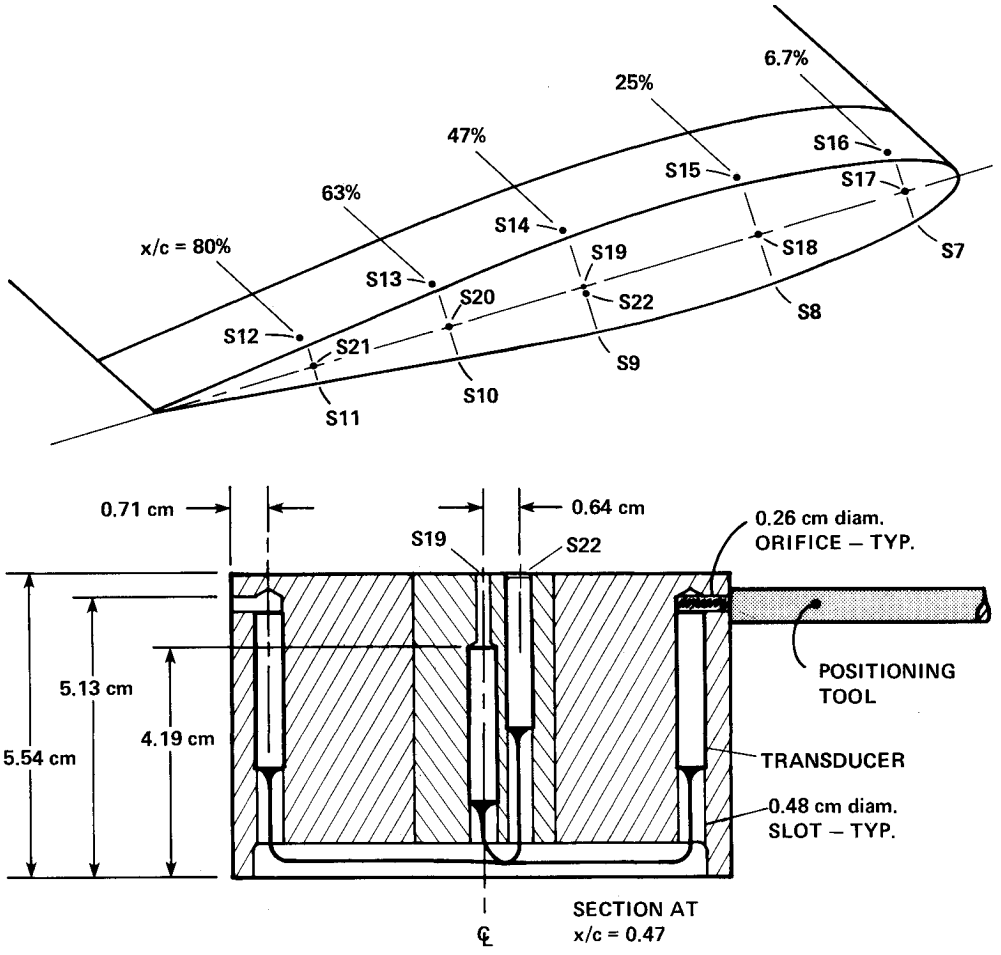

Fig. 2 Experimental model: a) sensor locations; b) cross-section of instrumented tip, only S22 was flush mounted.

spectra are indicated by dashed lines. In the spectra presented in the results, $E(f)$ is the pressure power spectral density.

When the cross spectrum of two signals can be approximated as a rectangular distribution of width Δf, centered on the peak frequency f_p, the cross correlation takes the form

$$\rho(\tau) \sim \cos[2\pi f_p(\tau - t_d)]\{\sin[\pi \Delta f(\tau - t_d)]/\pi \Delta f(\tau - t_d)\} \quad (1)$$

Table 1 Rms pressures normalized by the freestream head, $p^1(\rho U_0/2)$

Transducer	$\alpha = 16$ deg	$\alpha = 12$ deg	$\alpha = 6$ deg
S7	0.015	0.016	0.012
S8	0.014	0.012	(0.007)
S9	0.014	0.010	(0.006)
S10	0.011	(0.0090)	—
S11	(0.0074)	(0.0072)	—
S12	0.032	—	—
S13	0.047	0.024	(0.009)
S14	(0.014)	—	(0.018)
S15	(0.030)	0.029	(0.028)
S16	0.061	—	—
S17	0.025	0.025	0.024
S18	(0.081)	0.036	(0.007)
S22	0.097	0.082	(0.010)
S20	0.069	0.061	0.020
S21	0.032	0.028	0.016
S23	(0.007)	—	—
C_L	0.89	0.71	0.37
C_d	0.095	0.060	0.016

Values in parentheses are considered less reliable. Refer to text.

This form is based on the assumption that the two signals differ in phase only due to the delay time t_d. The quantity in braces will be referred to as the correlation envelope.

In boundary-layer studies, the delay time, t_d, for propogation between streamwise transducers is used to calculate a turbulence convection velocity $U_c = X/t_d$, where X is the streamwise distance between transducers. In this study, the mean flow and turbulence are strongly three-dimensional. Despite this, Eq. (1) was used to assess the qualitative characteristics of the turbulence. The convection delay time was established by the peak of the correlation envelope. An equivalent, streamwise, group convection velocity, U_c, was calculated using this delay time and the chordwise transducer separation distance. The peak of the correlation envelope was determined graphically.

Correlations were normalized using full rms pressures, although the signals were high-passed before correlation. The rms pressures used for normalization were calculated from Table 1.

Experimental Errors

A detailed explanation of the sources of experimental error can be found in Ref. 9. The uncertainty in absolute PSD levels is less than 1.5 dB if not otherwise noted. Dimensionless spectra given in dashed lines are those subject to greater uncertainty, as noted.

Random error in a correlation depends on the magnitude of the correlation coefficient, the number of averages, and the significant bandwidth of the data.[10] In the present case, this error is much less than the uncertainty in the rms levels used for normalization.

Results

Space limitations prevent a complete presentation of the data obtained. Emphasis is given to those spectra and cross correlations that best characterize the turbulence opposite the flat tip. Rms pressures normalized by the freestream head are presented in Table 1. Values given in parentheses are those subject to greater uncertainty. For reference, wing lift and induced drag coefficients estimated on the basis of finite wing theory[11,12] are also given in Table 1.

Spectra

Figures 3–9 present dimensionless spectra measured at angles of attack of 6, 12, and 16 deg. At the higher angles of attack, the S17 spectra, Fig. 3, did not collapse as well as others on the assumed characteristic variables. In correlation analyses, the energy in the low-frequency peak was found to be unrelated to all but the lower intensity S7 pressure fluctuations.

The spectra of S16, S17, and S7 measured at an angle of attack of 16 deg are shown in Fig. 4. These spectra show little similarity, even though all of the transducers were located at $x/c = 6.7\%$ (see Fig. 2). The pressure fluctuations at S16 were correlated only with those of S15 and S14 (downstream on the low pressure side of the wing) at all angles of attack. The double peaks in the spectrum of S16 in Fig. 4 at $\alpha = 16$ deg and in the spectrum of S7 at 12 deg in Fig. 5 are similar to those of vortex breakdown, velocity spectra measured by Garg and Leibovich,[13] although this may be coincidental. The pronounced peak in the spectra of S7 and S8 at 6 deg was not seen in other transducers on the high pressure side of the wing.

The dramatic increase in rms pressure levels on the flat tip, relative to those on the high pressure side of the wing, is immediately evident in Fig. 7. It is interesting to note that at 16 deg the PSD levels measured at S14 (not shown) on the low pressure side of the wing were as low as those of S9. Both of these transducers were within 4.0 cm of S22, where the most violent pressure fluctuations were measured at 16 deg. One might expect that the cross-flow pattern at this chordwise location was similar to that of Fig. 1b, cross-section B-B.

In Fig. 7, at 16 deg, the spectral levels at S13 on the low pressure side of the wing are greater than those of S21 on the flat tip. At 12 deg, Fig. 8, this situation is reversed. Although not shown in Fig. 9, the pressure levels at S13 were even lower at 6 deg. In contrast to the higher angles of attack, at 6 deg the pressure fluctuations at S13 were well correlated with the upstream transducers on the low pressure side of the wing, S15 and S14, and poorly correlated with those upstream on the flat tip. These observations are consistent with a secondary tip-vortex, cross-over position that moves downstream as the wing angle of attack decreases.

It is unfortunate that S12, the transducer on the low

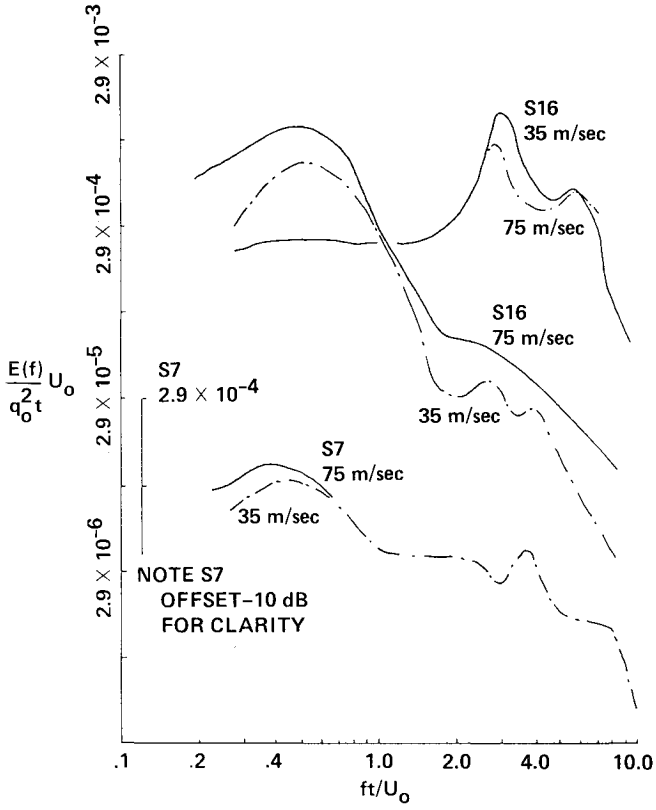

Fig. 4 Spectra of S7, S17, and S16 at an angle of attack of 16 deg.

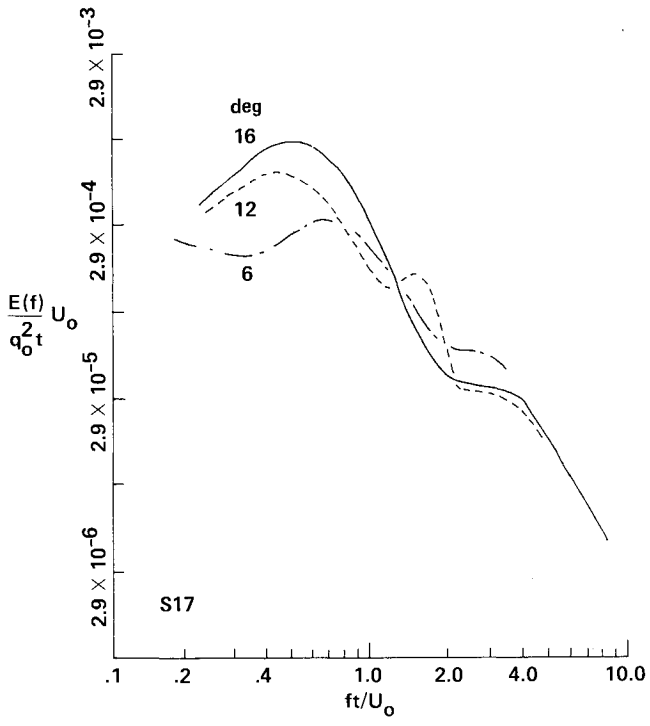

Fig. 3 Spectra of S17 at wing angles of attack of 16, 12, and 6 deg.

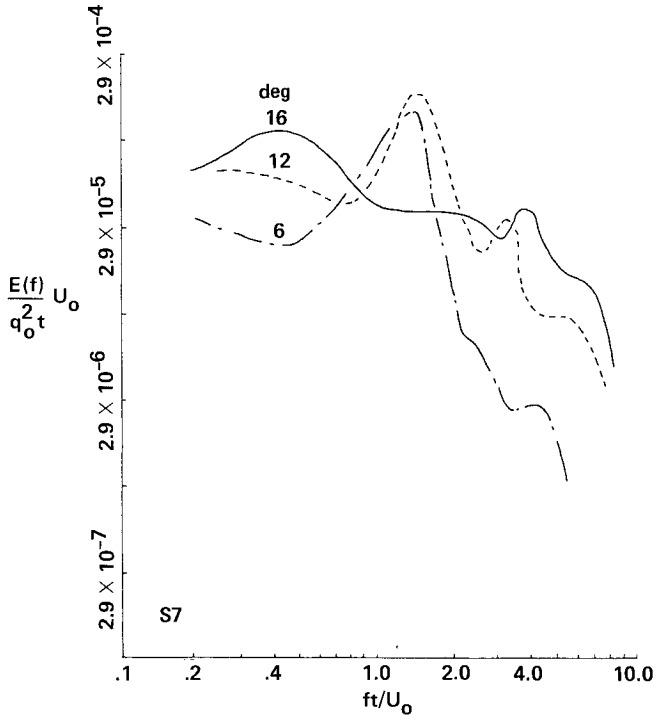

Fig. 5 Spectra of S7 at wing angles of attack of 16, 12, and 6 deg.

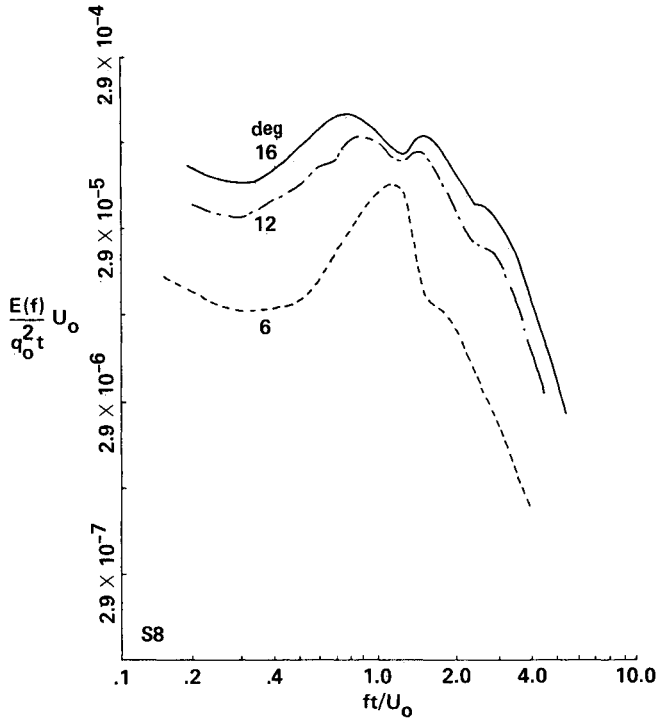

Fig. 6 Spectra of S8 at wing angles of attack of 16, 12, and 6 deg.

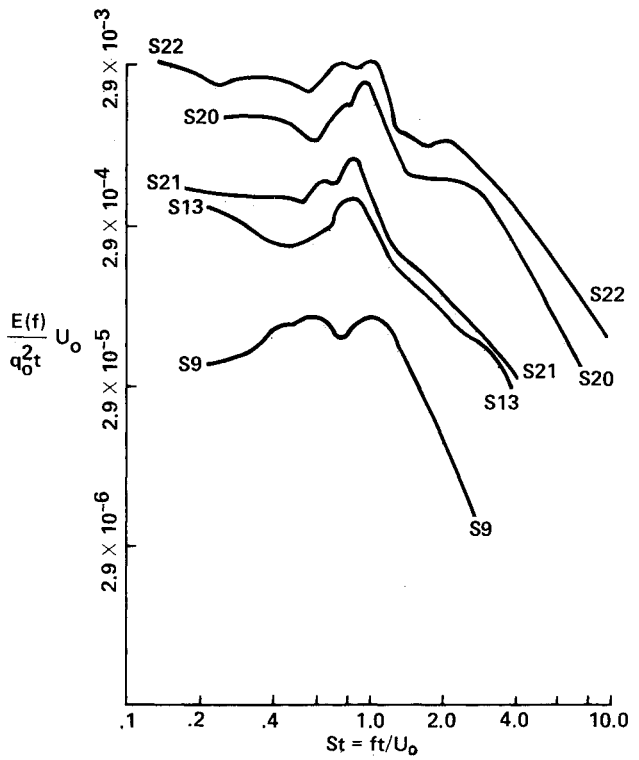

Fig. 8 Five spectra at a wing angle of attack of 12 deg.

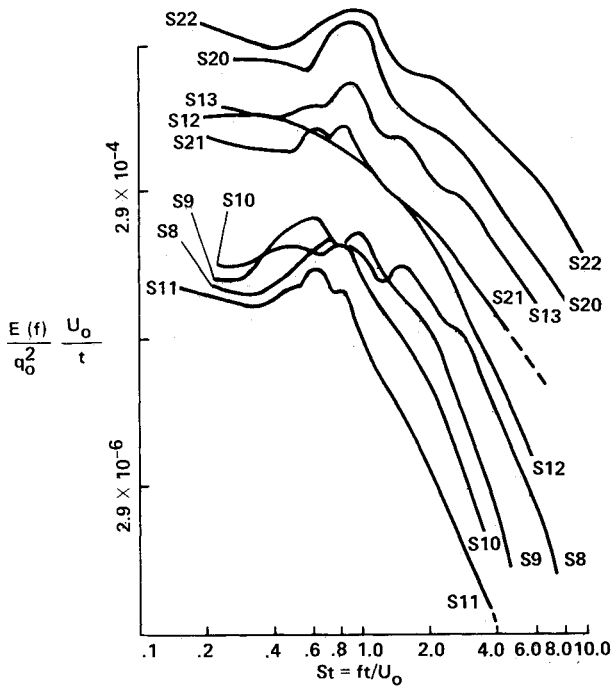

Fig. 7 Nine spectra at a wing angle of attack of 16 deg.

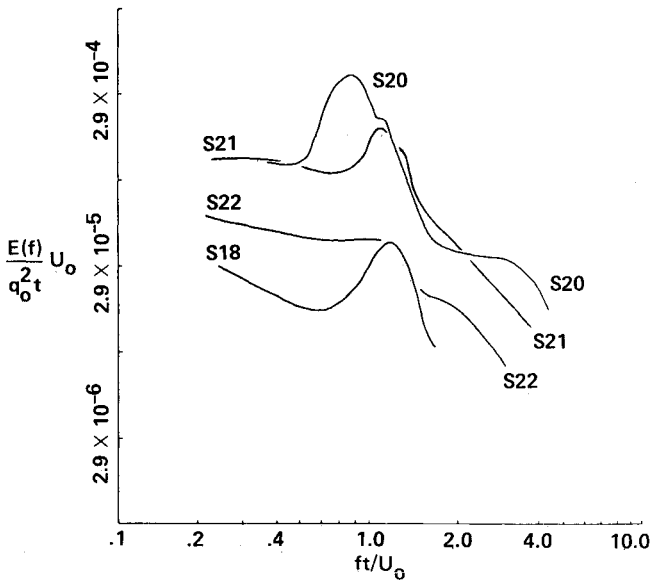

Fig. 9 Four spectra at a wing angle of attack of 6 deg.

pressure side of the wing nearest the trailing edge, failed to function at the lower angles of attack. The spectrum of S12 at 16 deg in Fig. 7 indicates high level, broadband turbulence on the corner of the wing near the trailing edge. This spectrum is dissimilar to those measured on the flat tip and upstream on the low pressure side of the wing. In Fig. 1, both tip-vortex axes are located about a wing thickness above the wing at this location and angle of attack.

The dimensionless spectra of S18, S22, and S20 at all three angles of attack are shown in Fig. 10. These have been plotted by adding 17 dB to the $\alpha = 6$ deg spectra and 5 dB to the 12-deg levels. A possible explanation for this data collapse is as follows. Assuming that pressure fluctuations under the secondary tip vortex are proportional to the wing induced drag, their dependence on wing angle of attack can be estimated from the coefficient of induced drag. Using lifting line theory[11,12] $C_d = C_L^2/[\pi AR]$. With $C_L = 2\pi\alpha/(1+2/AR)$, pressure power spectral density levels in dB ($10\ \mathrm{Log}_{10} < p^{12} >$) are predicted to vary as $20\ \mathrm{Log}_{10} \propto^2$. This crude analysis ignores the division of vorticity between primary and secondary tip vortices and presumes that S18, S22, and S20 were located directly underneath the secondary vortex axis at 16, 12, and 6 deg. Nonetheless, the spectra of S18, 22, 20, and 13 (not shown) show a promising degree of collapse over the range of $\alpha = 6$–16 deg.

Cross Correlations

Figure 11 is a cross correlation of transducers S8 and S22 at an angle of attack of 16 deg. This correlation displays the double structure seen between pressures measured near the (presumed) location of the secondary tip-vortex axis. Based on the chordwise separation, the convection velocities for the first and second groupings are $1.3U_0$ and $0.6U_0$, respectively. The corresponding Strouhal numbers ($f_p t/U_0$) are 1.5 and 0.75. The correlation of S18 with S13 was weaker, with a peak correlation coefficient of 0.08, but showed a similar structure with convection velocities of $1.1U_0$ and $0.67U_0$ and Strouhal numbers of 1.3 and 0.84. Transducer S7 was weakly correlated with all but S17 at this angle of attack.

The correlation of S22 and S20 at 16 deg is shown in Fig. 12. This represents the strongest, absolute pressure correlation measured between any two locations at all angles of attack. At 16 deg, S20 was not in close proximity to the secondary vortex axis, and this correlation does not show an echo-type structure. The correlation is suprisingly narrow-band, with $\Delta f = 0.67 f_p$ and $f_p t/U_0 = 0.83$. (The group convection velocity, using the chordwise separation distance, is $1.0U_0$. However, at 16 deg, it is unlikely that the mean flow was parallel to the chord line upon which these transducers were located.)

At 12 deg, the correlations of S7 with S18, S22, S13, and S21 all showed the dual-group structure. In these correlations the velocity of the second, lower frequency grouping increased with increasing separation distance, while the velocity of the first grouping decreased. The strength and peak frequency of the first grouping also tended to decrease more rapidly than that of the second as the separation distance was increased. Figure 13 shows the correlation of S7 and S22 at 12 deg. The two groupings in this correlation have Strouhal numbers of 1.4 and 1.0 and group convection velocities of 1.3 and $0.6U_0$.

None of the correlations for $\alpha = 6$ deg displayed a double grouping. At this angle of attack, the correlations of S7 with S18, S22, S20, and S21 presented a puzzling pattern. The peak correlation coefficients in the S7-S18, S7-S22, S7-S20, and S7-S21 correlations were 0.27, 0.09, 0.23, and 0.10, respectively. The corresponding group convection velocities were 0.93, 0.70, 1.0, and 0.70. The peak Strouhal numbers were all between 1.0 and 1.1. It is believed that this pattern is explained by the proximity of the individual transducers to the secondary vortex axis and the relatively low levels of boundary-layer turbulence at S18. The correlation of S7 and S20 at $\alpha = 6$ deg is shown in Fig. 14. The strength of this correlation, together with the $\alpha = 6$ deg spectra of S7 (see Fig. 5) and S20 (see Fig. 9), indicate that these transducers were located very near the secondary tip-vortex axis. The peak frequency of the energy in this correlation corresponds to a $St = 1.0$; the group convection velocity is $1.0U_0$.

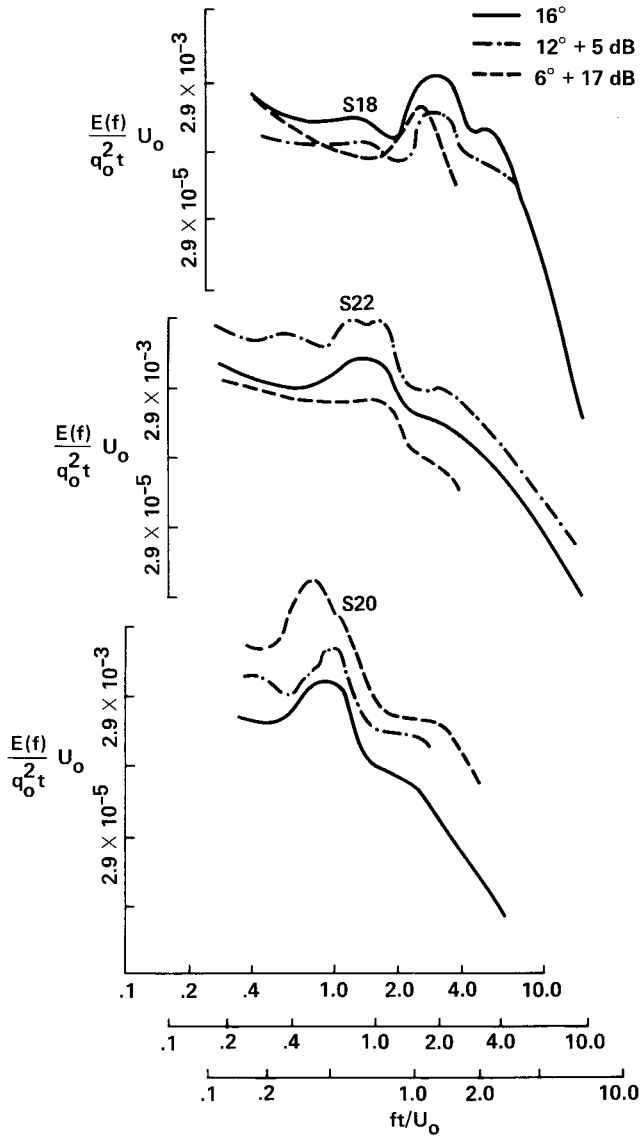

Fig. 10 Spectra of S18, S22, and S20 at 16, 12, and 6 deg.

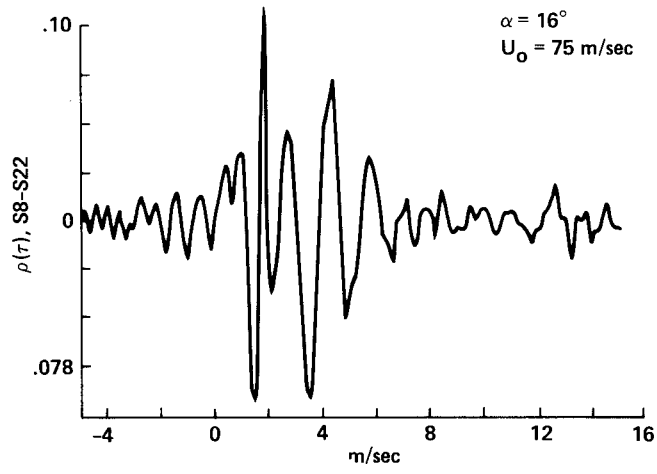

Fig. 11 Correlation of S8 and S22 at $\alpha = 16$ deg and $U_0 = 75$ m/s. Bandpass settings correspond to St 0.12–3.9.

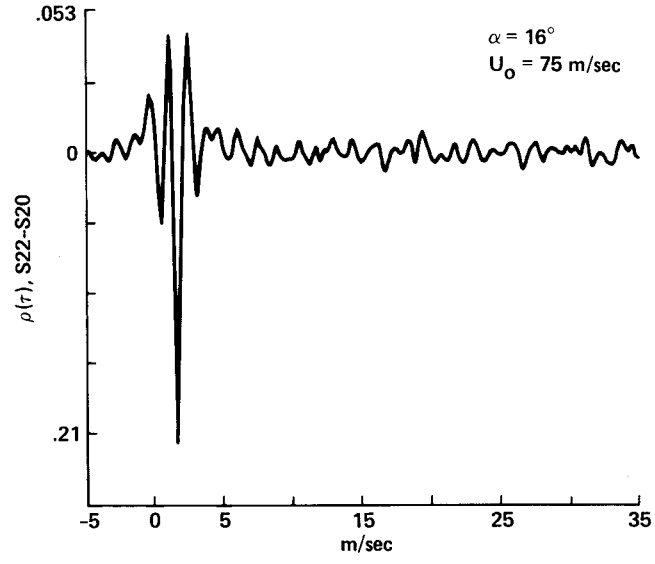

Fig. 12 Correlation of S20 and S22 at $\alpha = 16$ deg and $U_0 = 75$ m/s. Bandpass settings correspond to St 0.12–3.9.

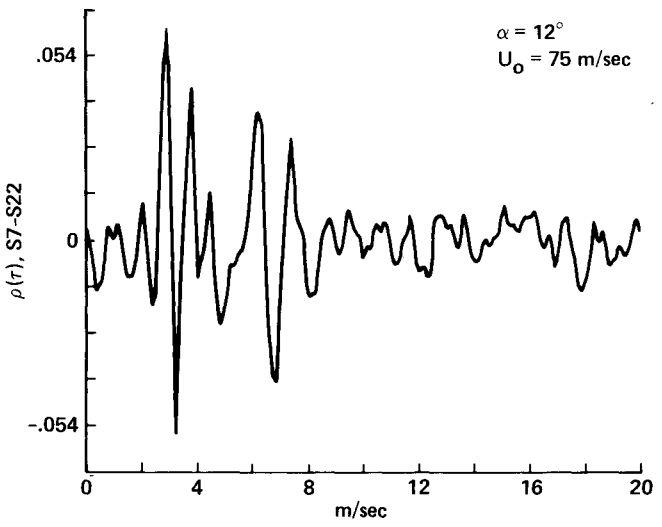

Fig. 13 Correlation of S7 and S22 at $\alpha = 12$ deg and $U_0 = 75$ m/s. Bandpass settings correspond to St 0.12-3.9.

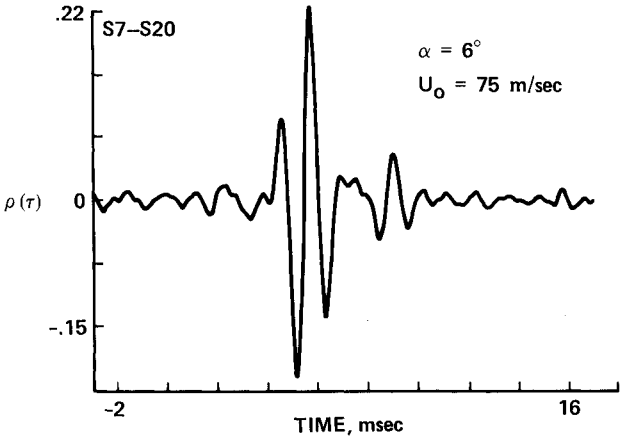

Fig. 14 Correlation of S7 and S20 at $\alpha = 6$ deg and $U_0 = 75$ m/s. Bandpass settings correspond to St 0.55-3.9.

Model

On the basis of the measured surface pressure fluctuations, it appears that the primary and secondary tip-vortex flows do not begin to interact until the secondary tip-vortex axis crosses the upper tip edge. The two steady tip vortices form independently, the primary tip vortex forming along the upper-tip edge and the secondary tip vortex along the lower edge, opposite the blunt tip. Taken together, the spectra and cross correlations presented here suggest the following model for the high level, relatively narrow-band turbulence associated with the secondary tip vortex.

At the sharp, lower-tip edge, unsteady vortices are shed into the circumferential flow leaving the high pressure side of the wing. These unsteady vortices are incorporated into the secondary tip-vortex flow and swept downstream. The core of this tip vortex is a relatively confined region of high-velocity, high-intensity turbulence. Since the axis of this tip-vortex core remains nearly parallel to the freestream velocity until it crosses the upper tip edge, the core remains close to the lower edge over most of the wing chord at an angle of atttack of 6 deg. At higher angles of attack, the core does not remain close to the lower tip edge. As a result, unsteady vortices shed at the lower tip edge are not completely ingested into the secondary tip-vortex core. That part of the resulting turbulence trapped within the vortex core is convected dowstream at a speed in excess of the freestream. The remainder moves downstream in the slower flow outside the vortex core. The difference in convection velocities for the two components of the turbulence provides an explanation for the echo-type cross correlations between transducers located near the secondary tip-vortex axis.

An alternate explanation for the dual groupings in the cross correlations was also considered. In this model, the two groupings were associated with convected turbulence (the slower moving disturbance) and with large-scale motion of the secondary tip vortex itself. The position of the tip vortex is known to fluctuate. However, large scale motion of this type would be almost immediately sensed at downstream locations and cannot account for the measured correlation delay times.

Conclusions

The results of an experimental study of surface pressure fluctuations in the tip region of a blunt tip airfoil have been presented. These include auto-spectral densities and cross correlations. Spectra measured at a fixed location and angles of attack display pronounced peaks at dimensionless frequencies, ft/U_0, on the order of one. As a function of angle of attack, pressure fluctuations measured on the flat tip, near the presumed location of the secondary tip vortex, collapsed reasonably well when the rms pressures were assumed proportional to the induced drag on the wing. A model for turbulence opposite the flat tip has been suggested. This model is capable of explaining the echo like cross correlations measured between transducers located near the core of the secondary tip vortex.

On the basis of the measured surface pressure characteristics and a limited number of hot-wire measurements made at $\alpha = 12$ deg (not reported here), an estimate of the scale of the turbulence opposite the flat tip can be made. The scale of the more slowly moving turbulence appears to have been on the order of one-third the wing thickness. Using $t/3$ as the characteristic length scale, the predominant peak frequency ($f_p t/U_0 = 0.8$) corresponds to a dimensionless frequency, $f_p(t/3)/U_0 = 0.27$. The frequency of the more rapidly convected turbulence should be made dimensionless using the mean streamwise velocity in the secondary tip-vortex core, U_m, and the core diameter, D. Neither of these was directly measured. A rough estimate can be made if it is assumed that $fD/U_m = 0.25$ and the measured convection velocity was $0.8U_m$. With $U_m = 1.3U_0/0.8$ and $ft/U_0 = 1.4$ from S7-S22 at 12 deg (see Fig. 13), the diameter of the secondary tip-vortex core is also estimated to be one-third the wing thickness.

Acknowledgment

This work was supported by the Low Speed Aircraft Research Branch of the NASA Ames Research Center.

References

[1]Meecham, W. C., "Theory of Airframe Noise," *Journal of the Acoustical Society of America,* Vol. 57, No. 6, Pt II, June 1975, pp. 1416-1420.

[2]Fink, M. R., and Schlinker, R. H., "Airframe Noise Component Interaction Studies," AIAA Paper 79-0668, March 1979.

[3]Miller, W. R., Meecham, W. C., and Ahtye, W. F., "Large Scale Model Measurements of Airframe Noise Using Cross-Correlation Techniques," *Journal of the Acoustical Society of America,* Vol. 71, Pt 3, March 1981, pp. 591-599.

[4]Kendall, J. M., and Ahtye, W. F., "Noise Generation by a Lifting Wing/Flap Combination at Reynolds Numbers to 2.8 × 106," AIAA Paper 80-0035, Jan. 1980.

[5]Francis, M. S., and Kennedy, D. A., "Formation of a Trailing Vortex," *Journal of Aircraft,* Vol. 16, No. 3, March 1979, pp. 148-154.

[6]Chigier, N. A., and Corsiglia, V. R., "Tip Vortices-Velocity Distributions," NASA TM X-62,087, Sept. 1971.

[7]Shivananda, T. P., McMahon, J. M., and Gray, R. B., "Surface Pressure Measurements at the Tip of a Model Helicopter Rotor in Hover," *Journal of Aircraft*, Vol. 15, No. 8, Aug. 1978, pp. 460–467.
[8]Hoffman, J. D. and Velkoff, J. R., "Vortex Flow over Helicoptor Rotor Tips," *Journal of Aircraft*, Vol. 8, No. 9, Sept. 1971, pp. 739–740.
[9]McInerny, S. A., "An Experimental Investigation of Wing-Tip Turbulence and Sound Radiated from the Tip Region of a Blunt-Tipped Airfoil," Ph.D. Disssertation, Mechanical, Aerospace and Nuclear Engineering Department, Univ. of California, Los Angeles, March 1987.
[10]Bendat, J. S. and Piersol, A. G., *Engineering Applications of Correlation and Spectral Analysis*, Wiley, New York, 1961.
[11]Kuethe, A. M. and Chow, C. -Y., *Foundations of Aerodynamics*, 3rd ed., Wiley, New York, 1976.
[12]Abbot, I. H. and Von Doenhoff, A. E., *Theory of Wing Sections*, Dover, New York, 1959.
[13]Garg, A. K. and Leibovich, S., "Spectral Characteristics of Vortex Breakdown Flowfields," *Physics of Fluids*, Vol. 22, No. 11, Nov. 1979, pp. 2053–2064.